Catal Lett (2009) 130:192–197
DOI 10.1007/s10562-009-9854-9

Production of Middle Distillate from Synthesis Gas in a Dual-bed Reactor Through Hydrocracking of Wax Over Mesoporous Pd-Al_2O_3 Composite Catalyst

**Insung Nam · Kyung Min Cho · Jeong Gil Seo ·
Sunhwan Hwang · Ki-Won Jun · In Kyu Song**

Received: 2 January 2009 / Accepted: 5 January 2009 / Published online: 17 January 2009

Abstract Production of middle distillate (C_{10}–C_{20}) from synthesis gas ($CO + H_2$) through hydrocracking of wax ($>C_{21+}$) was carried out in a dual-bed reactor. Co/TiO_2 catalyst was used in the first-bed reactor to produce wax from synthesis gas, and a mesoporous Pd-alumina composite catalyst (Pd-Al_2O_3) was used in the second-bed reactor to produce middle distillate through hydrocracking of wax. For comparison, a Pd catalyst supported on mesoporous alumina (Pd/Al_2O_3) was also examined as a second-bed catalyst. The catalytic performance of Pd-Al_2O_3 and Pd/Al_2O_3 for hydrocracking of wax to middle distillate was tested and compared. It was revealed that selectivity for middle distillate in the dual-bed reactor was much higher than that in the first-bed reactor, indicating that both Pd-Al_2O_3 and Pd/Al_2O_3 catalysts in the second-bed reactor served as an efficient catalyst for hydrocracking of wax to middle distillate. Furthermore, Pd-Al_2O_3 catalyst showed a higher selectivity for middle distillate than Pd/Al_2O_3. The enhanced catalytic performance of Pd-Al_2O_3 for hydrocracking of wax to middle distillate was due to high Pd dispersion and high Pd surface area. Large medium acidity of Pd-Al_2O_3 catalyst was also responsible for its high catalytic performance in the hydrocracking of wax to middle distillate.

Keywords Middle distillate · Hydrocracking of wax · Fischer–Tropsch synthesis · Mesoporous Pd-Al_2O_3 catalyst

1 Introduction

Hydrocracking is a key process in petroleum refining for the conversion of heavy hydrocarbons into high value and low boiling point products such as gasoline and diesel [1–3]. Hydrocracking also allows the conversion of a wide range of feedstocks to a variety of products [2]. In particular, hydrocracking has been widely studied in the hybrid Fischer–Tropsch synthesis for the production of gasoline (C_5–C_{11}) and middle distillate (C_{10}–C_{20}) [4–13].

A conventional dual-bed reactor system for the production of middle distillate (C_{10}–C_{20}) from synthesis gas ($CO + H_2$) through hydrocracking of wax ($>C_{21+}$) is composed of two serial reactions; a low-temperature Fischer–Tropsch synthesis for the production of long-chain hydrocarbon (wax) from synthesis gas in the first-bed reactor, and a subsequent hydrocracking of wax into middle distillate in the second-bed reactor [10]. In the dual-bed reactor system for the production of middle distillate, Fischer–Tropsch synthesis reaction in the first-bed reactor and hydrocracking reaction in the second-bed reactor are operated independently. Therefore, selective production of middle distillate from synthesis gas can be attained by changing the catalyst and reaction conditions in the dual-bed reactor system.

Hydrocracking is generally conducted over a metal/acid bifunctional catalyst. Alkanes are dehydrogenated on the metallic sites and then isomerized or cracked on the acid sites through classical or non-classical carbenium ion chemistry [11, 14–16]. Although Ni-W and Ni-Mo oxides supported on solid acids have been conventionally used for

---

I. Nam · K. M. Cho · J. G. Seo · S. Hwang · I. K. Song (✉)
School of Chemical and Biological Engineering, Institute of Chemical Processes, Seoul National University, Shinlim-dong, Kwanak-ku, Seoul 151-744, South Korea
e-mail: inksong@snu.ac.kr

K.-W. Jun
Korea Research Institute of Chemical Technologies, Taejon 305-600, South Korea

the production of middle distillate through hydrocracking of wax [17], Pd-loaded solid acid catalysts have also been widely employed for hydrocracking of wax because they show a high activity for hydrocracking of sulfur-free heavy hydrocarbons [12, 13, 18]. Acid property of metal/acid bifunctional catalyst is very important to obtain high selectivity for middle distillate in the hydrocracking of wax. It has been reported that selectivity for middle distillate increases with increasing medium acidity of the catalyst [12, 13]. Metal dispersion in the catalyst also plays an important role in achieving high selectivity for middle distillate in the hydrocracking of wax. It is known that dehydrogenation function of metal/acid bifunctional catalyst is enhanced by increasing metal dispersion of the catalyst in the hydrocracking of wax [19]. Therefore, it is expected that selectivity for middle distillate in the hydrocracking of wax would be much enhanced, if a metal/acid bifunctional catalyst retains large medium acidity and high metal dispersion.

In this work, Co/TiO_2 catalyst prepared by an incipient wetness impregnation method was used as a Fischer–Tropsch catalyst for the production of wax from synthesis gas in the first-bed reactor. A mesoporous Pd-alumina composite catalyst (Pd-Al_2O_3) prepared by a surfactant-templating method was applied to the production of middle distillate through hydrocracking of wax in the second-bed reactor. For comparison, a Pd catalyst supported on mesoporous alumina (Pd/Al_2O_3) prepared by an impregnation method was also employed as a second-bed catalyst. The catalytic performance of Pd-Al_2O_3 and Pd/Al_2O_3 for hydrocracking of wax to middle distillate in the second-bed reactor was extensively investigated.

2 Experimental

2.1 Preparation of Co/TiO_2 Catalyst

About 15 wt% Co/TiO_2 was prepared by an incipient wetness impregnation method for use as a Fischer–Tropsch synthesis catalyst in the first-bed reactor. Cobalt nitrate ($Co(NO_3)_2 \cdot 6H_2O$, Sigma–Aldrich) was used as a cobalt precursor, and TiO_2 (P25, Degussa) was used as a support. The prepared Co/TiO_2 catalyst was calcined at 300 °C for 20 h [20].

2.2 Preparation of Pd-Al_2O_3 and Pd/Al_2O_3 Catalysts

A mesoporous Pd-Al_2O_3 was prepared by an anionic surfactant-templating method, according to the similar method reported in the literature [21]. About 3 g of anionic surfactant (lauric acid, Sigma–Aldrich) was dissolved in 30 ml of 1-propanol (Sigma–Aldrich) at room temperature under constant stirring to yield a micelle solution (Solution A). 17.4 g of aluminum precursor (aluminum *sec*-butoxide, Sigma–Aldrich) was then separately dissolved in 30 ml of 1-propanol at room temperature under constant stirring (Solution B). After adding Solution B into Solution A, the resulting solution was stirred for 2 h to obtain a micelle-aluminum precursor complex (Solution C). Another solution containing known amount of palladium precursor ($Pd(NO_3)_2$, Sigma–Aldrich) and 2.75 ml of distilled water was diluted with 17.5 ml of 1-propanol (Solution D). A semi-solid solution of palladium precursor-micelle-aluminum precursor complex was formed within a few seconds upon adding Solution D into Solution C. After stirring the semi-solid solution for 2 h, it was maintained at 100 °C for 24 h. The solid obtained by centrifugation was successively washed with ethanol and distilled water. The solid product was dried overnight at 80 °C, and then it was calcined at 800 °C for 5 h to yield the mesoporous Pd-Al_2O_3. The mesoporous Pd-alumina composite catalyst was denoted as Pd-Al_2O_3.

A mesoporous alumina was prepared according to the reported method [21, 22] for use as a supporting material for Pd catalyst. Preparation procedures for mesoporous alumina were almost identical to those of Pd-Al_2O_3, expect that palladium precursor was not used in the preparation of mesoporous alumina. A Pd catalyst supported on mesoporous alumina was then prepared by impregnating known amount of palladium precursor ($Pd(NO_3)_2$, Sigma–Aldrich). After drying the impregnated catalyst overnight at 80 °C, it was calcined at 500 °C for 5 h. The Pd catalyst supported on mesoporous alumina was denoted as Pd/Al_2O_3. Pd loading was fixed at 0.6 wt% in both Pd-Al_2O_3 and Pd/Al_2O_3 catalysts.

2.3 Characterization

Nitrogen adsorption–desorption isotherms of Pd-Al_2O_3 and Pd/Al_2O_3 catalysts were obtained with an ASAP-2010 (Micrometrics) instrument, and pore size distributions were determined by the BJH (Barret–Joyner–Hallender) method applied to the desorption branch of the isotherms. Hydrogen chemisorption experiments (BELCAT-B, BEL Japan) were conducted to measure the Pd dispersion and Pd surface area of the catalysts. Prior to the chemisorption measurements, 50 mg of each catalyst was reduced with a mixed stream of hydrogen (2.5 ml/min) and argon (47.5 ml/min) at 400 °C for 3 h, and subsequently, it was purged with pure argon (50 ml/min) for 15 min at 400 °C. The sample was then cooled to 50 °C under a flow of argon (50 ml/min). The amount of hydrogen uptake was determined by periodically injecting diluted hydrogen (5% hydrogen and 95% argon) into the reduced catalyst using an on-line sampling valve. Pd dispersion and Pd surface area were calculated by assuming that one hydrogen atom occupies one surface Pd atom and that cross-sectional area of atomic Pd is 7.87 × 10^{-20} m^2/Pd-atom. Acid properties of Pd-Al_2O_3 and Pd/Al_2O_3 catalysts were measured by NH_3-TPD experiments (BELCAT-B, BEL Japan). Prior to the NH_3-TPD experiments, 50 mg of each catalyst was reduced with a mixed stream of hydrogen (2.5 ml/min) and argon (47.5 ml/min) at 400 °C for 3 h. The sample was then cooled to 50 °C under a flow of helium (50 ml/min). Diluted ammonia (5% hydrogen and 95% helium) was introduced into the reactor for 30 min at 50 °C to saturate acid sites with ammonia. The physisorbed ammonia was removed by evacuating the catalyst sample at 50 °C for 10 min. Furnace temperature was increased from 50 to 1,000 °C at a heating rate of 10 °C/min under a flow of helium (30 ml/min). The desorbed ammonia was detected using a TCD. The amount of carbon deposition in the used catalysts was determined by CHNS elemental analyses (CHNS 932, Leco).

2.4 Catalytic Reaction

The reaction was carried out in a dual-bed fixed-bed reactor. Both first-bed and second-bed reactors (SUS, ID = 8 mm) were consecutively arranged in the vertical direction. In the first-bed reactor, a Fischer–Tropsch catalyst (Co/TiO_2) was loaded to produce long-chain hydrocarbon (wax). In the second-bed reactor, either Pd-Al_2O_3 or Pd/Al_2O_3 was loaded for hydrocracking of wax from the first-bed reactor. 0.3 g of Co/TiO_2 catalyst diluted with 0.5 g of quartz sand was charged in the first-bed reactor. The Fischer–Tropsch synthesis reaction in the first-bed reactor was conducted under the conditions of $P = 12$ bar, $H_2/CO = 2.0$, $W/F = 20.0$ g-cat-h/mol, and $T = 220$ °C. 0.3 g of either Pd-Al_2O_3 or Pd/Al_2O_3 was used in the second-bed reactor. Additional H_2 was introduced into the second-bed reactor, where H_2/CO ratio was fixed at 2.5 by assuming no reaction in the first-bed reactor. The reaction in the second-bed reactor was conducted under the conditions of $P = 12$ bar and $T = 330$ °C. Prior to the reaction, the first-bed catalyst (Co/TiO_2) was reduced at 250 °C for 16 h and the second-bed catalyst (either Pd-Al_2O_3 or Pd/Al_2O_3) was reduced at 400 °C for 16 h. All the reaction experiments were conducted more than 24 h under the steady-state condition.

Effluent hydrocarbon products which were not condensed at a hot trap were analyzed using an on-line GC (HP 5890II, Agilent) equipped with a FID. CO, CH_4, and CO_2 in the effluent stream from a water trap were analyzed using a GC (Younglin, 600D) equipped with a TCD, and light hydrocarbons (C_1–C_5) in the effluent stream were also analyzed using a GC (Younglin, 600D) equipped with a FID. Heavy hydrocarbon products (C_{10+}) collected from a hot trap were analyzed using a GC (HP 5890II, Agilent) equipped with a FID. The reaction data in each reactor were obtained after a 10 h-reaction. For more accurate analysis, the liquid product was collected for 10 h without sampling. CO conversion and hydrocarbon selectivity were calculated according to the following equations.

$$\text{CO conversion}(\%) = \frac{(\text{weight of CO introduced}) - (\text{weight of CO unreacted})}{(\text{weight of CO introduced})} \tag{1}$$

$$\text{Hydrocarbon selectivity (wt\%)} = \frac{(\text{weight of specific hydrocarbon produced})}{(\text{weight of total hydrocarbon produced})} \tag{2}$$

3 Results and Discussion

3.1 Textural Property of Pd-Al_2O_3 and Pd/Al_2O_3 Catalysts

Textural properties of Pd-Al_2O_3 and Pd/Al_2O_3 catalysts were examined by nitrogen adsorption–desorption isotherm measurements. Figure 1 shows the nitrogen adsorption–desorption isotherms and pore size distributions of Pd-Al_2O_3 and Pd/Al_2O_3 catalysts. Both Pd-Al_2O_3 and Pd/Al_2O_3 catalysts clearly showed IV-type isotherms with H_2-type hysteresis loops, indicating the existence of well-developed framework mesopores [21, 22]. Surface areas, pore volumes, and average pore diameters of Pd-Al_2O_3 and Pd/Al_2O_3 catalysts are summarized in Table 1. Pd-Al_2O_3 catalyst showed high surface area and large pore volume

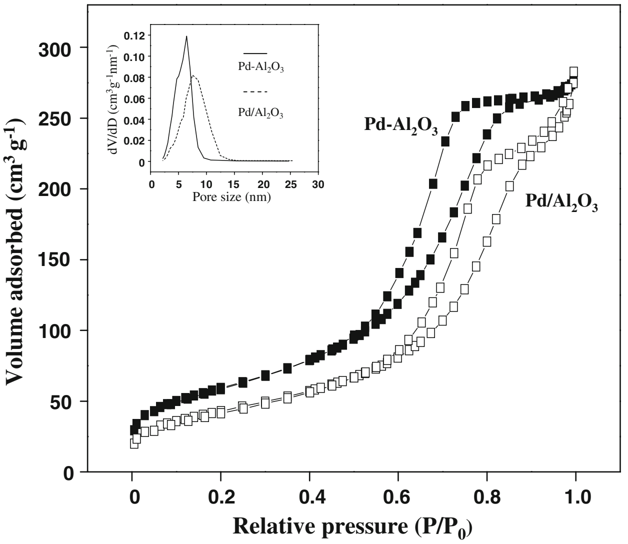

Fig. 1 Nitrogen adsorption–desorption isotherms and pore size distributions of Pd-Al_2O_2 and Pd/Al_2O_3 catalysts

Table 1 Textural properties of Pd-Al_2O_3 and Pd/Al_2O_3 catalysts

	Surface area (m^2/g)[a]	Pore volume (cm^3/g)[b]	Average pore diameter (nm)[c]
Pd-Al_2O_3	214	0.41	5.3
Pd/Al_2O_3	157	0.37	6.7

[a] Calculated by the BET (Brunauer–Emmett–Teller) equation

[b] BJH (Barret–Joyner–Hallender) desorption pore volume

[c] BJH (Barret–Joyner–Hallender) desorption average pore diameter

compared to Pd/Al_2O_3 catalyst. Average pore diameters of Pd-Al_2O_3 and Pd/Al_2O_3 catalysts were found to be 5.3 nm and 6.7 nm, respectively. The smaller average pore size of Pd-Al_2O_3 catalyst is believed to be due to the incorporated Pd species which retarded the dehydroxylation and sintering reactions of alumina particles during the calcination step through the formation of Pd-O–Al composite structure [21].

3.2 Catalytic Performance in the Dual-bed Reactor

It is desired to produce heavy hydrocarbons (middle distillate and wax) through Fischer–Tropsch synthesis in the first-bed reactor. In this work, Co/TiO_2 was used as an efficient catalyst for the first-bed reactor [13]. Table 2 shows the catalytic performance of Co/TiO_2 for Fischer–Tropsch synthesis in the first-bed reactor. Co/TiO_2 catalyst showed high selectivity's for middle distillate (36.5 wt%) and wax (29.9 wt%). This means that these products can be utilized as a suitable feed for the production of middle distillate through hydrocracking in the second-bed reactor.

Figure 2 shows the carbon number distributions of liquid product (C_{10+}) in the first-bed reactor (Co/TiO_2) and in the dual-bed reactor (Co/TiO_2 + Pd-Al_2O_3). Figure 2 clearly shows that wax produced in the first-bed reactor was mainly hydrocracked to middle distillate. Table 3 shows the carbon number distributions over Pd-Al_2O_3 and Pd/Al_2O_3 catalysts in the second-bed reactor. selectivity's for methane and light hydrocarbons (C_2–C_4) in the dual-bed reactor were somewhat increased compared to those in the first-bed reactor, indicating the occurrence of hydrocracking in the second-bed reactor. Direct comparison of Tables 2 and 3 revealed that selectivity for middle distillate in the dual-bed reactor was much higher than that in the first-bed reactor. This means that both Pd-Al_2O_3 and Pd/Al_2O_3 catalysts served as an efficient catalyst for hydrocracking of wax to middle distillate. The increments of middle distillate selectivity over Pd-Al_2O_3 and Pd/Al_2O_3 catalysts were found to be 12.6 wt% (= 49.1 − 36.5 wt%) and 9.4 wt% (= 45.9 − 36.5 wt%), respectively. This indicates that Pd-Al_2O_3 catalyst was more efficient than Pd/Al_2O_3 catalyst for the production of middle distillate through hydrocracking of wax.

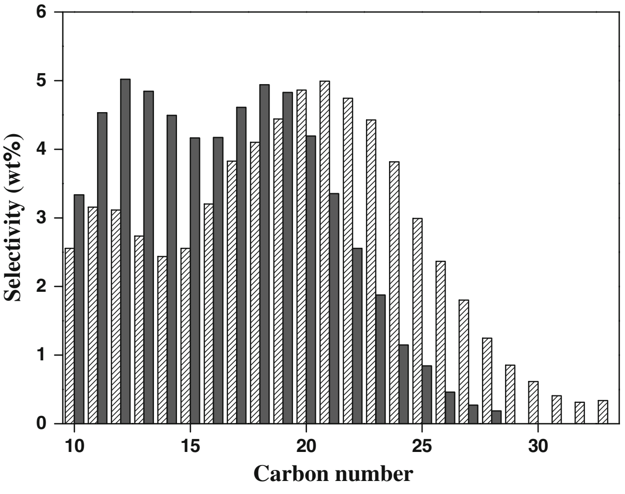

Fig. 2 Carbon number distributions in the first-bed reactor and in the dual-bed reactor ▨ = Co/TiO_2 (first-bed only), ■ = CO/TiO_2 (first-bed) + Pd-Al_2O_3 (second-bed)

Table 3 Carbon number distributions over Pd-Al_2O_3 and Pd/Al_2O_3 catalysts in the second-bed reactor

Catalyst	Hydrocarbon selectivity (wt%)				
	C_1	C_2–C_4	C_{10}–C_{20}	C_{21+}	C_{5+}
Pd-Al_2O_3	8.5	6.0	49.1	10.7	85.5
Pd/Al_2O_3	5.4	5.9	45.9	23.8	91.0

3.3 Palladium Dispersion and Palladium Surface Area

In order to elucidate the different catalytic performance between Pd-Al_2O_3 and Pd/Al_2O_3, hydrogen chemisorption measurements were conducted. Pd dispersion and Pd surface area of Pd-Al_2O_3 and Pd/Al_2O_3 catalysts determined by hydrogen chemisorption experiments are listed in Table 4. Table 4 clearly shows that Pd dispersion and Pd surface area of Pd-Al_2O_3 catalyst were much higher than

Table 2 Catalytic performance of Co/TiO_2 for Fischer–Tropsch synthesis in the first-bed reactor

Catalyst	CO conversion (%)	Hydrocarbon selectivity (wt%)					Chain growth probability (α)[a]
		C_1	C_2–C_4	C_{10}–C_{20}	C_{21+}	C_{5+}	
Co/TiO_2	84.6	4.6	5.4	36.5	29.9	90.0	0.89

[a] Calculated within the range of C_{10}–C_{22}

Table 4 Hydrogen chemisorption results for Pd-Al_2O_3 and Pd/Al_2O_3 catalysts

	Amount of H_2 uptake (μmol/g-catalyst)	Pd dispersion (%)	Pd surface Area (m^2/g-Pd)[a]
Pd-Al_2O_3	3.7	13.1	58.4
Pd/Al_2O_3	2.4	8.5	37.9

[a] Calculated by assuming H/Pd_{atom} = 1

those of Pd/Al_2O_3 catalyst. This means that palladium species were more homogeneously dispersed in the Pd-Al_2O_3 catalyst. It can be inferred that micelle with anionic charge was successfully bonded to positively charged palladium precursor and aluminum precursor in the preparation of Pd-Al_2O_3 catalyst. This (palladium precursor)$^+$(micelle)$^-$(aluminum precursor)$^+$ complex was then transformed into Pd-O–Al composite material upon removal of surfactant through the calcination process [21]. Thus, palladium species were more finely dispersed in the Pd-Al_2O_3 catalyst through the formation of favorable Pd-O–Al composite structure. High Pd dispersion and high Pd surface area improves the hydrogenation–dehydrogenation activity of Pd for hydrocarbons [19]. Therefore, it is believed that the enhanced catalytic performance of Pd-Al_2O_3 in the hydrocracking of wax to middle distillate was due to its high Pd dispersion and high Pd surface area.

3.4 Acid Property of Pd-Al_2O_3 and Pd/Al_2O_3 Catalysts

In order to investigate the effect of acid property of Pd-Al_2O_3 and Pd/Al_2O_3 catalysts on their catalytic performance in the second-bed reactor, NH_3-TPD measurements were carried out. Figure 3 shows the NH_3-TPD profiles of Pd-Al_2O_3 and Pd/Al_2O_3 catalysts, and Fig. 4 shows the deconvoluted TPD profiles of Pd-Al_2O_3 catalyst. Deconvolution of TPD profile reveals that there are three types of acid sites. A low-temperature peak in the range of 120–190 °C, a medium-temperature peak in the range of 220–290 °C, and a high-temperature peak in the range of 550–680 °C correspond to weak, medium, and strong acid sites, respectively. Acidities of Pd-Al_2O_3 and Pd/Al_2O_3 catalysts are summarized in Table 5. It should be noted that Pd-Al_2O_3 catalyst retained larger medium acidity than Pd/Al_2O_3 catalyst. It has been previously reported that the increment of middle distillate selectivity in the second-bed reactor increases with increasing medium acidity of the catalyst [12, 13]. It is also known that the reaction rate is accelerated by the medium acid sites of the catalyst in the monomolecular reaction (the cracking of carbonium ion formed by protonation of feed molecule) [23–25]. Therefore, it is believed that the enhanced catalytic performance of Pd-Al_2O_3 in the hydrocracking of wax to middle distillate was also due to its large medium acidity.

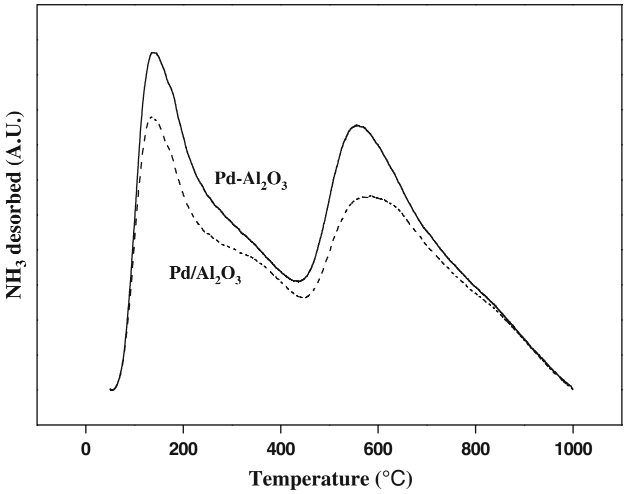

Fig. 3 NH_3-TPD profiles of Pd-Al_2O_2 and Pd/Al_2O_3 catalysts

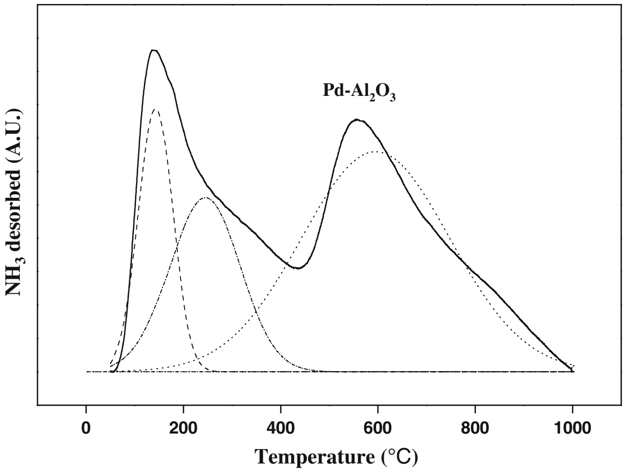

Fig. 4 Deconvoluted TPD profiles of Pd-Al_2O_3 catalyst

3.5 Catalyst Stability

Table 6 shows the amount of carbon deposited on Pd-Al_2O_3 and Pd/Al_2O_3 catalysts after 24 h-reaction. The amount of carbon deposited on Pd-Al_2O_3 catalyst was smaller than that on Pd/Al_2O_3 catalyst. Carbon deposition preferentially occurs on the surface of large metal particles,

Table 5 Acidities of Pd-Al_2O_3 and Pd/Al_2O_3 catalysts

Catalyst	Acidity (mmol NH_3/g-catalyst)			
	Weak acid site (120–190 °C)	Medium acid site (220–290 °C)	Strong acid site (550–680 °C)	Total acidity
Pd-Al_2O_3	0.10	0.15	0.39	0.64
Pd/Al_2O_3	0.08	0.13	0.33	0.54

Table 6 Amount of carbon deposited on Pd-Al_2O_3 and Pd/Al_2O_3 catalysts after 24 h-reaction

	Pd-Al_2O_3	Pd/Al_2O_3
Amount of carbon deposition (wt%)[a]	0.850	1.688

[a] Determined by CHNS elemental analysis

and small metal particles have strong resistance toward carbon deposition. The above result indicates that Pd-Al_2O_3 catalyst with higher Pd dispersion than Pd/Al_2O_3 catalyst served as a more stable catalyst in the hydrocracking of wax.

4 Conclusions

Selective production of middle distillate (C_{10}–C_{20}) from synthesis gas ($CO + H_2$) through hydrocracking of wax ($>C_{21+}$) was carried out in a dual-bed reactor. Co/TiO_2 catalyst was used in the first-bed reactor to produce wax from synthesis gas. Either Pd-Al_2O_3 catalyst prepared by an anionic surfactant-templating method or Pd/Al_2O_3 catalyst prepared by an impregnation method was used in the second-bed reactor to produce middle distillate through hydrocracking of wax. The catalytic performance of Pd-Al_2O_3 and Pd/Al_2O_3 for hydrocracking of wax to middle distillate in the second-bed reactor was investigated. Selectivity for middle distillate in the dual-bed reactor was found to be much higher than that in the first-bed reactor, representing that both Pd-Al_2O_3 and Pd/Al_2O_3 catalysts in the second-bed reactor acted as an efficient catalyst for hydrocracking of wax to middle distillate. The increments of middle distillate selectivity over Pd-Al_2O_3 and Pd/Al_2O_3 catalysts were 12.6 and 9.4 wt%, respectively, indicating that Pd-Al_2O_3 catalyst was more efficient than Pd/Al_2O_3 catalyst for the production of middle distillate through hydrocracking of wax. The enhanced catalytic performance of Pd-Al_2O_3 for hydrocracking of wax to middle distillate was due to its high Pd dispersion and high Pd surface area. Large medium acidity of Pd-Al_2O_3 catalyst was also responsible for its high catalytic performance in the hydrocracking of wax to middle distillate.

Acknowledgments The authors would like to acknowledge the financial support of KEMCO and GTL Technology Development Consortium (Korea National Oil Corp., Daelim Industrial Co. LTD, Doosan Mecatec Co. LTD, Hyundai Engineering Co. LTD, and SK Energy Co. LTD) under “Energy & Resources Technology Development Programs” of the Ministry of Knowledge Economy, Republic of Korea (2006-11-0133-3-020).

References

1. Konoval’chikov LD, Nefedov BK, Kruglikov VY, Konoval’chikov OD (1984) Chem Tech Fuels Oils 20:8–11
2. Scherzer J, Gruia AJ (1996) Hydrocracking science and technology. Marcel Dekker, New York
3. Keogh RA, Sparks D, Hu J, Wender I, Tierney JW, Wang W, Davis BH (1994) Energy Fuels 8:755–762
4. Liu ZW, Li X, Asami K, Fujimoto K (2005) Catal Today 104:41–47
5. de Klerk A (2008) Catal Today 130:439–445
6. Li X, Asami K, Luo M, Michiki K, Tsubaki N, Fusimoto K (2003) Catal Today 84:59–65
7. Martinez A, Valencia A, Murciano R, Cerqueira HS, Costa AF, Aguiar EFS (2008) Appl Catal A Gen 346:117–125
8. Liu ZW, Li X, Asami K, Fujimoto K (2005) Energy Fuels 19:1790–1794
9. Liu ZW, Li X, Asami K, Fujimoto K (2005) Catal Commun 6:503–506
10. Zhao TS, Chang J, Yoneyama Y, Tsubaki N (2005) Ind Eng Chem Res 44:769–775
11. Sie ST (1993) Ind Eng Chem Res 32:403–408
12. Cho KM, Park S, Seo JG, Youn MH, Baeck S-H, Jun K-W, Chung JS, Song IK (2008) Appl Catal B Environ 83:195–201
13. Cho KM, Park S, Seo JG, Youn MH, Nam I, Baeck S-H, Jun K-W, Chung JS, Song IK (2008) Chem Eng J 146:307–314
14. Mills GA, Heinemann H, Milliken TH, Oblad AG (1953) Ind Eng Chem Res 45:134–142
15. Venkatesh KR, Hu J, Wang W, Holder GD, Tierney JW, Wender I (1996) Energy Fuels 10:1163–1170
16. Liu ZW, Li X, Asami K, Fujimoto K (2000) Appl Catal A Gen 197:191–200
17. Hwang S, Lee J, Park S, Park DR, Jung JC, Lee S-B, Song IK (2008) Catal Lett doi:10.1007/s10562-008-9784-y
18. Grunes J, Zhu J, Yang M, Somorjai GA (2003) Catal Lett 86:157–161
19. Angevine PJ, Huang TJ (2000) PCT WO 00/40333
20. Madikizela-Mngangeni NN, Coville NJ (2005) J Mol Catal A Chem 225:137–142
21. Seo JG, Youn MH, Park S, Park DR, Jung JC, Chung JS, Song IK (2008) Catal Today doi:10.1016/j.cattod.2008.12.008
22. Ray JC, You K-S, Ahn J-W, Ahn WS (2007) Micropor Mesopor Mater 100:183–190
23. Songip AR, Masuda T, Kuwahara H, Hashimoto K (1994) Energy Fuels 8:136–140
24. de la Puente G, Sedran UA (1998) J Catal 179:36–42
25. Jolly J, Saussey J, Bettahar MM, Lavalley JC, Benazzi E (1997) Appl Catal A Gen 156:71–96